Supplementary Material (21 pages)

On the Relationship between Sensitivity Coefficients and Transfer Functions in Reaction Kinetic Networks

Tormod Drengstig[1], **Thomas Kjosmoen**[1] **and Peter Ruoff**[2]
[1]*Department of Electrical Engineering and Computer Science, University of Stavanger, N-4036 Stavanger, Norway;* [2]*Centre for Organelle Research, University of Stavanger, N-4036 Stavanger, Norway*

Stoichiometric Network Approach

A frequency domain approach to sensitivity analysis was formulated by Ingalls [1] based on stoichiometric network theory [2], describing a kinetic system as:

$$\dot{\mathbf{s}}(t) = \mathbf{N}\mathbf{v}\big(\mathbf{s}(t), \mathbf{p}(t)\big) \tag{A1}$$

where $\mathbf{s}(t)$, $\mathbf{v}(t)$ and $\mathbf{p}(t)$ are vectors of species concentrations, reaction rates, rate constants and other internal/external parameters, respectively, and the matrix $\mathbf{N}$ describes the stoichiometry of the system. The stoichiometric network model given by Eq. A1 can be written as a linear time-invariant input-output system as by Eq. 3 in main paper with the system matrix $A = \mathbf{N_R}\frac{\partial \mathbf{v}}{\partial \mathbf{s}}\mathbf{L}$ and the input matrix $B = \mathbf{N_R}\frac{\partial \mathbf{v}}{\partial \mathbf{p}}$. The matrix $\mathbf{L}$ is the *link matrix* and $\mathbf{N_R}$ is the *reduced stoichiometric matrix* consisting of the independent rows of $\mathbf{N}$, i.e. $\mathbf{N} = \mathbf{L}\mathbf{N_R}$ [1, 2]. The inputs are the reaction rates.

The model output from Eq. A1 can be expressed similarly to the network properties described by Eq. 4 in main paper. If the stoichiometric network model output is related to concentrations, then $C = I$ and $D = 0$ in the generalized state space model. On the other hand, if the stoichiometric network model output is related to fluxes, then $C = \frac{\partial \mathbf{v}}{\partial \mathbf{s}}\mathbf{L}$ and $D = \frac{\partial \mathbf{v}}{\partial \mathbf{p}}$. Hence, the calculation of the matrices C and D depends on the actual property (flux or concentration) and is not generic as in our state space approach. Therefore, instead of one generic expression for the transfer function (as Eq. 5 in main paper), two different expressions for the transfer functions are needed (please note that Eqs. 9 and 10 in Ref. [1] contain misprints, which are corrected here):

$$\mathbf{H}_{\mathbf{s_i}}(s) = \left(sI - \mathbf{N_R}\frac{\partial \mathbf{v}}{\partial \mathbf{s}}\mathbf{L}\right)^{-1}\mathbf{N_R}\frac{\partial \mathbf{v}}{\partial \mathbf{p}} \tag{A2}$$

$$\mathbf{H}_{\mathbf{v}}(s) = \frac{\partial \mathbf{v}}{\partial \mathbf{s}}\mathbf{L}\left(sI - \mathbf{N_R}\frac{\partial \mathbf{v}}{\partial \mathbf{s}}\mathbf{L}\right)^{-1}\mathbf{N_R}\frac{\partial \mathbf{v}}{\partial \mathbf{p}} + \frac{\partial \mathbf{v}}{\partial \mathbf{p}} \tag{A3}$$

The transfer functions $\mathbf{H}_{\mathbf{s_i}}(s)$ and $\mathbf{H}_{\mathbf{v}}(s)$ are for concentration and flux model outputs, respectively.

Furthermore, Ingalls [1] defines the transfer functions in Eqs. A2 and A3 to be the same as frequency dependent unscaled (absolute) *concentration* and *rate response coefficients*, respectively, i.e. $\mathbf{R}_{\mathbf{s_i}}(s) = \mathbf{H}_{\mathbf{s_i}}(s)$ and $\mathbf{R}_{\mathbf{v}}(s) = \mathbf{H}_{\mathbf{v}}(s)$. Based on these definitions and the generic relationship between the absolute response coefficients $\mathbf{R}^{\mathbf{x}}_{\mathbf{p}} = \frac{\partial \mathbf{x}}{\partial \mathbf{p}}$, the absolute control coefficients $\mathbf{C}^{\mathbf{x}}_{\mathbf{v}} = \frac{\partial \mathbf{x}}{\partial \mathbf{v}}$ and the absolute elasticity coefficients $\epsilon^{\mathbf{v}}_{\mathbf{p}} = \frac{\partial \mathbf{v}}{\partial \mathbf{p}}$, defined as $\mathbf{R}^{\mathbf{x}}_{\mathbf{p}} = \mathbf{C}^{\mathbf{x}}_{\mathbf{v}}\epsilon^{\mathbf{v}}_{\mathbf{p}}$ in Ref. [3], Ingalls [1] relates the transfer function and the unscaled/absolute control coefficients as:

$$\mathbf{H}_{\mathbf{s_i}}(s) = \mathbf{C}_{\mathbf{s_i}}(s)\frac{\partial \mathbf{v}}{\partial \mathbf{p}} \tag{A4}$$

$$\mathbf{H}_{\mathbf{v}}(s) = \mathbf{C}_{\mathbf{v}}(s)\frac{\partial \mathbf{v}}{\partial \mathbf{p}} \tag{A5}$$

where the frequency dependent unscaled/absolute *concentration* and *flux control coefficients* can be found as:

$$\mathbf{C}_{\mathbf{s_i}}(s) = \left(sI - \mathbf{N_R}\frac{\partial \mathbf{v}}{\partial \mathbf{s}}\mathbf{L}\right)^{-1}\mathbf{N_R} \tag{A6}$$

$$\mathbf{C}_{\mathbf{v}}(s) = \frac{\partial \mathbf{v}}{\partial \mathbf{s}}\mathbf{L}\left(sI - \mathbf{N_R}\frac{\partial \mathbf{v}}{\partial \mathbf{s}}\mathbf{L}\right)^{-1}\mathbf{N_R} + I \tag{A7}$$

In order to compare these specific results with the general result from Eq. 13 in main paper, we need the *relative* concentration and flux control coefficient matrices given as (from Hofmeyr [3])

$$\tilde{\mathbf{C}}_{\mathbf{s_i}}(s) = (D^{s_i})^{-1}\cdot\mathbf{C}_{\mathbf{s_i}}(s)\cdot D^{v} \tag{A8}$$

$$\tilde{\mathbf{C}}_{\mathbf{v}}(s) = (D^{v})^{-1}\cdot\mathbf{C}_{\mathbf{v}}(s)\cdot D^{v} \tag{A9}$$

where $D^v = \mathrm{diag}\big(v(s_i^0, p^0)\big)$ and $D^{s_i} = \mathrm{diag}(s_i^0)$, and s_i^0 and p^0 are the steady state values of species concentration and parameters, respectively [1].

As opposed to the state space approach, the dimensions of the two matrices $\mathbf{H_{s_i}}(s)$ and $\mathbf{C_{s_i}}(s)$ (or $\mathbf{H_v}(s)$ and $\mathbf{C_v}(s)$) may actually differ since $\frac{\partial \mathbf{v}}{\partial \mathbf{p}}$ may not be square (i.e. when using lumped reaction rates in the modeling), and therefore impossible to compare elementwise. The steady state relative concentration/flux control coefficients $\tilde{\mathbf{C}}_{\mathbf{s_i}}$ and $\tilde{\mathbf{C}}_{\mathbf{v}}$ are found by setting $s = 0$ in Eqs. A8 and A9, respectively.

To summarize, the state space approach described in main paper can find *any* relative sensitivity coefficient by first identifying the transfer function matrix (Eq. 5 in main paper), either by modeling or a system identification method, and then use the single relationship in Eq. 13 shown in main paper. The stoichiometric network approach is an alternative way to identify the relative concentration/flux control coefficient matrices. There are, however, limitations (lack of generality) to the stoichiometric network approach compared to the state space method:

- The choice of output (flux or concentration) determines which transfer function ($\mathbf{H_{s_i}}(s)$ or $\mathbf{H_v}(s)$) to be used.
- Only reaction rates v are used as input.
- The stoichiometric network approach cannot be applied when numerical (not symbolic) A, B, C and D matrices or transfer functions have been obtained by a system identification approach, because the matrices $\mathbf{N_R}$, D^v, D^{s_i} and $\frac{\partial \mathbf{v}}{\partial \mathbf{p}}$ require knowledge of the model structure.
- Similarly, if only a transfer function (symbolic or numerical) exists for a reaction network where an input is considered to be lumped by two or more reactions, the matrix $\frac{\partial \mathbf{v}}{\partial \mathbf{p}}$ is not invertible. Hence, the control coefficient matrices $\mathbf{C_{s_i}}(s)$ and $\mathbf{C_v}(s)$ cannot be found by using Eqs. A4 and A5.

Illustrating the principles

As mentioned in the main paper, we use three different motifs to illustrate the scenarios describing the different kinds of adaptation. We use supscript $^{\mathbf{1}}$, $^{\mathbf{2}}$, $^{\mathbf{3}}$, $^{\mathbf{4}}$ or $^{\mathbf{5}}$ to indicate which matrix element is robustly disconnected (scenario 1), non-robustly disconnected (scenario 2), robust perfectly adapted (scenario 3), non-robust perfectly adapted (scenario 4) or near non-robust perfectly adapted (scenario 5), respectively.

Motif M1

Motif M1 presented in the main paper is shown below

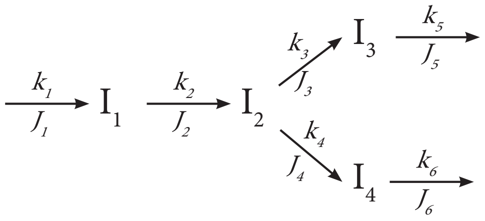

(M1)

where each rate constant depends on temperature using the Arrhenius equation as $k_n(t) = A_n{\cdot}e^{\frac{-E_n}{RT(t)}}$. The nonlinear dynamic model for motif M1 becomes:

$$\frac{dx_1(t)}{dt} = A_1{\cdot}e^{\frac{-E_1}{RT(t)}} - A_2{\cdot}e^{\frac{-E_2}{RT(t)}}{\cdot}x_1(t) \tag{A10}$$

$$\frac{dx_2(t)}{dt} = A_2{\cdot}e^{\frac{-E_2}{RT(t)}}{\cdot}x_1(t) - A_3{\cdot}e^{\frac{-E_3}{RT(t)}}{\cdot}x_2(t) - A_4{\cdot}e^{\frac{-E_4}{RT(t)}}{\cdot}x_2(t) \tag{A11}$$

$$\frac{dx_3(t)}{dt} = A_3{\cdot}e^{\frac{-E_3}{RT(t)}}{\cdot}x_2(t) - A_5{\cdot}e^{\frac{-E_5}{RT(t)}}{\cdot}x_3(t) \tag{A12}$$

$$\frac{dx_4(t)}{dt} = A_4{\cdot}e^{\frac{-E_4}{RT(t)}}{\cdot}x_2(t) - A_6{\cdot}e^{\frac{-E_6}{RT(t)}}{\cdot}x_4(t) \tag{A13}$$

producing the following linear state space matrices A and B:

$$A = \begin{bmatrix} -A_2{\cdot}e^{\frac{-E_2}{RT}} & 0 & 0 & 0 \\ A_2{\cdot}e^{\frac{-E_2}{RT}} & -\left(A_3{\cdot}e^{\frac{-E_3}{RT}} + A_4{\cdot}e^{\frac{-E_4}{RT}}\right) & 0 & 0 \\ 0 & A_3{\cdot}e^{\frac{-E_3}{RT}} & -A_5{\cdot}e^{\frac{-E_5}{RT}} & 0 \\ 0 & A_4{\cdot}e^{\frac{-E_4}{RT}} & 0 & -A_6{\cdot}e^{\frac{-E_6}{RT}} \end{bmatrix} \tag{A14}$$

$$B = \begin{bmatrix} \frac{A_1E_1}{RT^2}e^{\frac{-E_1}{RT}} - \frac{A_2x_1E_2}{RT^2}e^{\frac{-E_2}{RT}} \\ \frac{A_2x_1E_2}{RT^2}e^{\frac{-E_2}{RT}} - \frac{A_3x_2E_3}{RT^2}e^{\frac{-E_3}{RT}} - \frac{A_4x_2E_4}{RT^2}e^{\frac{-E_4}{RT}} \\ \frac{A_3x_2E_3}{RT^2}e^{\frac{-E_3}{RT}} - \frac{A_5x_3E_5}{RT^2}e^{\frac{-E_5}{RT}} \\ \frac{A_4x_2E_4}{RT^2}e^{\frac{-E_4}{RT}} - \frac{A_6x_4E_6}{RT^2}e^{\frac{-E_6}{RT}} \end{bmatrix} \tag{A15}$$

where the steady state values of the concentrations $\mathbf{x_{ss}}$ are

$$x_1 = \frac{A_1 \cdot e^{\frac{-E_1}{RT}}}{A_2 \cdot e^{\frac{-E_2}{RT}}} \tag{A16}$$

$$x_2 = A_1 \cdot e^{\frac{-E_1}{RT}} \cdot (A_3 \cdot e^{\frac{-E_3}{RT}} + A_4 \cdot e^{\frac{-E_4}{RT}}) \tag{A17}$$

$$x_3 = \frac{A_1 A_3 e^{\frac{E_5}{RT}}}{A_5 e^{\frac{E_1}{RT}} e^{\frac{E_3}{RT}} \left(A_3 e^{\frac{-E_3}{RT}} + A_4 e^{\frac{-E_4}{RT}} \right)} \tag{A18}$$

$$x_4 = \frac{A_1 A_4 e^{\frac{E_6}{RT}}}{A_6 e^{\frac{E_1}{RT}} e^{\frac{E_4}{RT}} \left(A_3 e^{\frac{-E_3}{RT}} + A_4 e^{\frac{-E_4}{RT}} \right)} \tag{A19}$$

Fluxes as model output

In this scenario, the input to the model is the scalar temperature $\mathbf{u}(t) = T(t)$ and the output from the model is the fluxes $\mathbf{y}(t) = [k_1(t),\ k_2(t)x_1(t),\ k_3(t)x_2(t),\ k_4(t)x_2(t),\ k_5(t)x_3(t),\ k_6(t)x_4(t)]^T$. The non-linear model in Eqs. A10-A13 is simulated using a step-wise increase of 10K in temperature from 308K to 318K at $t = 1$. The response in the fluxes $J_1(t), \ldots, J_6(t)$ is shown in Fig. S1. A comparison between the analytical (based on Eq. 30 in main paper) and the empirical (based on Eq. 10 in main paper and the responses in Fig. S1) steady state relative sensitivity coefficient matrices are shown in Eq. A20 (analytical to the left, empirical to the right):

$$\mathbf{C}_{\mathbf{u}}^{\mathbf{y}} = \begin{bmatrix} 0.02616 \\ 0.02616 \\ 0.04806 \\ 0.00975 \\ 0.04806 \\ 0.00975 \end{bmatrix}, \quad \mathbf{C}_{\mathbf{u}}^{\mathbf{y}} \approx \begin{bmatrix} 0.02535 \\ 0.02535 \\ 0.04653 \\ 0.00943 \\ 0.04653 \\ 0.00943 \end{bmatrix} \tag{A20}$$

As wee see, the values differs, and these differences are due to the relative large step of 10K in temperature increase. A smaller step-wise increase in temperature will reduce the difference, and this actually demonstrates the non-linearity of the system.

Concentration as model output

Using concentrations as model output, i.e. $\mathbf{y}(t) = [x_1(t),\ x_2(t),\ x_3(t),\ x_4(t)]^T$, the relative sensitivity coefficient matrix from temperature to concentration is

$$\mathbf{C}^{\mathbf{y}}_{\mathbf{u}} = \left(\begin{array}{c} \frac{E_1 - E_2}{RT}^{\mathbf{4}} \\ \frac{A_3 E_1 e^{\frac{-E_3}{RT}} - A_3\, E_3 e^{\frac{-E_3}{RT}} + A_4\, E_1 e^{\frac{-E_4}{RT}} - A_4\, E_4 e^{\frac{-E_4}{RT}}}{RT\left(A_3 e^{\frac{-E_3}{RT}} + A_4 e^{\frac{-E_4}{RT}}\right)}^{\mathbf{5}} \\ \frac{A_4\, E_3 e^{\frac{-E_4}{RT}} - A_4\, E_4 e^{\frac{-E_4}{RT}}}{RT\left(A_3 e^{\frac{-E_3}{RT}} + A_4 e^{\frac{-E_4}{RT}}\right)} + \frac{E_1}{RT} - \frac{E_5}{RT}^{\mathbf{5}} \\ \frac{E_1}{RT} - \frac{\left(A_3\, E_3 e^{\frac{-E_3}{RT}} - A_3\, E_4 e^{\frac{-E_3}{RT}}\right)}{RT\left(A_3 e^{\frac{-E_3}{RT}} + A_4 e^{\frac{-E_4}{RT}}\right)} - \frac{E_6}{RT}^{\mathbf{5}} \end{array} \right) \tag{A21}$$

which shows a combination of non-robust and near non-robust perfect adaptation sites. The conditions for near non-robust perfect adaptation of the elements $\mathbf{C}^{\mathbf{y}}_{\mathbf{u}}(2,1)$, $\mathbf{C}^{\mathbf{y}}_{\mathbf{u}}(3,1)$ and $\mathbf{C}^{\mathbf{y}}_{\mathbf{u}}(4,1)$ are:

$$A_3 e^{-\frac{E_3}{RT}}(E_1 - E_3) + A_4 e^{-\frac{E_4}{RT}}(E_1 - E_4) = 0 \tag{A22}$$

$$A_3 e^{-\frac{E_3}{RT}}(E_1 - E_5) + A_4 e^{-\frac{E_4}{RT}}(E_1 + E_3 - E_4 - E_5) = 0 \tag{A23}$$

$$A_3 e^{-\frac{E_3}{RT}}(E_1 - E_3 + E_4 - E_6) + A_4 e^{-\frac{E_4}{RT}}(E_1 - E_6) = 0 \tag{A24}$$

Comparing the 2 conditions from Eqs. 22 and 23 in main paper against the 3 conditions in Eqs. A22-A24, shows that it is impossible to obtain adaptation in any flux and in any concentration simultaneously.

Motif M2

Motif M2 (shown below) is used to illustrate and compare the generalized state space model approach (based on the left scheme in M2) with the stoichiometric network model approach (based on the right scheme in M2 where k_2 and k_{-2} are lumped into v_2) as described by Ingalls [1] using both concentrations and fluxes as model outputs.

$$\xrightarrow{k_1} \mathrm{I}_1 \underset{k_{-2}}{\overset{k_2}{\rightleftarrows}} \mathrm{I}_2 \xrightarrow{k_3} \qquad \xrightarrow{v_1} \mathrm{I}_1 \overset{v_2}{\rightleftarrows} \mathrm{I}_2 \xrightarrow{v_3} \tag{M2}$$

Concentrations as Model Output

State Space Model Approach

Using the state space model approach, the rate equations become

$$\frac{dx_1(t)}{dt} = k_1(t) - k_2(t)x_1(t) + k_{-2}(t)x_2(t) \tag{A25}$$

$$\frac{dx_2(t)}{dt} = k_2(t)x_1(t) - k_3(t)x_2(t) - k_{-2}(t)x_2(t) \tag{A26}$$

where the input vector is $\mathbf{u}(t) = [k_1(t),\ k_2(t),\ k_{-2}(t),\ k_3(t)]^T$ and the state vector is $\mathbf{x}(t) = [x_1(t),\ x_2(t)]^T$. Focusing first on concentrations as model output, the output vector becomes $\mathbf{y}(t) = [x_1(t),\ x_2(t)]^T$. This gives the following matrices for the linearized state space model

$$A = \begin{bmatrix} -k_2 & k_{-2} \\ k_2 & -(k_3 + k_{-2}) \end{bmatrix}, \quad B = \begin{bmatrix} 1 & -x_1 & x_2 & 0 \\ 0 & x_1 & -x_2 & -x_2 \end{bmatrix}$$

$$C = \begin{bmatrix} 1 & 0 \\ 0 & 1 \end{bmatrix}, \quad D = \begin{bmatrix} 0 & 0 & 0 & 0 \\ 0 & 0 & 0 & 0 \end{bmatrix}$$

Using the steady state expressions for the concentrations

$$\mathbf{x_{ss}} = [x_1, x_2]^T = \left[\frac{k_{-2}k_1 + k_1k_3}{k_3k_2},\ \frac{k_1}{k_3} \right]^T \tag{A27}$$

and the steady state expressions for the outputs, i.e. $\mathbf{y_{ss}} = [x_1,\ x_2]^T$, the transfer function matrix $\mathbf{H}(s)$ becomes:

$$\mathbf{H}(s) = \frac{1}{s^2 + s(k_2 + k_3 + k_{-2}) + k_3k_2} \cdot \begin{bmatrix} (s + k_{-2} + k_3) & \frac{-(s+k_3)k_1(k_{-2}+k_3)}{k_2k_3} & \frac{(s+k_3)k_1}{k_3} & \frac{-k_{-2}k_1}{k_3} \\ k_2 & \frac{sk_1(k_{-2}+k_3)}{k_2k_3} & -\frac{sk_1}{k_3} & -\frac{(s+k_2)k_1}{k_3} \end{bmatrix} \tag{A28}$$

The frequency dependent relative sensitivity coefficient matrix $\mathbf{C}^{\mathbf{y}}_{\mathbf{u}}(s)$ becomes:

$$\begin{aligned}
\mathbf{C}^{\mathbf{y}}_{\mathbf{u}}(s) =& \mathbf{H}(s) \circ \frac{\mathbf{u_{ss}}}{\mathbf{y_{ss}}} \\
=& \frac{1}{s^2 + s(k_2 + k_3 + k_{-2}) + k_3 k_2} \cdot \\
& \begin{bmatrix} \frac{(s+k_3+k_{-2})k_2k_3}{k_3+k_{-2}} & -(s+k_3)k_2 & \frac{(s+k_3)k_{-2}k_2}{k_3+k_{-2}} & \frac{-k_{-2}k_2k_3}{k_3+k_{-2}} \\ k_2k_3 & (k_3+k_{-2})s & -k_{-2}s & -(s+k_2)k_3 \end{bmatrix}
\end{aligned} \tag{A29}$$

where the functions of the numerator polynomial $n^{yp}_{un}(s)$ of e.g. element (2,2) are

$$q(\mathbf{u_{ss}}, \boldsymbol{\alpha}) = 1 \tag{A30}$$

$$h_1(\mathbf{u_{ss}}, \boldsymbol{\alpha}) = (k_3 + k_{-2}) \tag{A31}$$

$$h_0(\mathbf{u_{ss}}, \boldsymbol{\alpha}) = 0 \tag{A32}$$

fulfilling the conditions for scenario 3. Similar results are found for element (2,3), implying that component I_2 is robust perfectly adapted to step-wise changes in rate constants $k_2(t)$ and $k_{-2}(t)$. The steady state relative sensitivity coefficient matrix becomes:

$$\mathbf{C}^{\mathbf{y}}_{\mathbf{u}} = \begin{bmatrix} 1 & -1 & \frac{k_{-2}}{k_{-2}+k_3} & -\frac{k_{-2}}{k_{-2}+k_3} \\ 1 & 0^{\mathbf{3}} & 0^{\mathbf{3}} & -1 \end{bmatrix} \tag{A33}$$

The summation theorem applied to either of the steady state or frequency dependent relative sensitivity coefficient matrix matrices in Eqs. A29 or A33 gives (summed over all N reactions):

$$\sum_{all\ N} \mathbf{C}^{\mathbf{y}}_{\mathbf{u}} = \begin{bmatrix} 0 \\ 0 \end{bmatrix}$$

The $\mathbf{C}^{\mathbf{y}}_{\mathbf{u}}(s)$ matrix in Eq. A29 is presented in terms of Bode plots in Fig. S2, where the steady state properties of Eq. A33 can be found by inspecting the Bode plots as the frequency approaches 0. For example, the element (1,1) of Eq. A33 has a relative amplification of 1, which corresponds to $20 \cdot \log_{10}(1) = 0$ dB as shown in Fig. S2. Another example is the element (2,2) where the relative amplification approaches 0, i.e. $-\infty$ dB, whereas the element (1,3) has an amplification of $\frac{k_{-2}}{k_3+k_{-2}} = \frac{1.3}{1.4+1.3} = 0.48$, i.e. -6.35 dB,

Stoichiometric Network Model Approach

In order to find the corresponding relative concentration control coefficient matrix from the stoichiometric network model approach, we use the following velocity vector:

$$\mathbf{v} = \begin{bmatrix} v_1 \\ v_2 \\ v_3 \end{bmatrix} = \begin{bmatrix} k_1 \\ k_2 s_1 - k_{-2} s_2 \\ k_3 s_2 \end{bmatrix} \tag{A34}$$

where s_1 and s_2 denote concentrations x_1 and x_2, respectively. Using

$$\frac{\partial \mathbf{v}}{\partial \mathbf{s}} = \begin{bmatrix} 0 & 0 \\ k_2 & k_{-2} \\ 0 & k_3 \end{bmatrix}, \quad \mathbf{N} = \mathbf{N_R} = \begin{bmatrix} 1 & -1 & 0 \\ 0 & 1 & -1 \end{bmatrix}, \quad \frac{\partial \mathbf{v}}{\partial \mathbf{p}} = \begin{bmatrix} 1 & 0 & 0 & 0 \\ 0 & s_1 & -s_2 & 0 \\ 0 & 0 & 0 & s_2 \end{bmatrix} \tag{A35}$$

the transfer function matrix $\mathbf{H_{si}}(s)$ becomes

$$\begin{aligned} \mathbf{H_{si}}(s) = & \frac{1}{s^2 + s(k_2 + k_3 + k_{-2}) + k_3 k_2} \cdot \\ & \begin{bmatrix} (s + k_{-2} + k_3) & \frac{-(s+k_3)k_1(k_{-2}+k_3)}{k_2 k_3} & \frac{(s+k_3)k_1}{k_3} & \frac{-k_{-2}k_1}{k_3} \\ k_2 & \frac{s k_1(k_{-2}+k_3)}{k_2 k_3} & -\frac{s k_1}{k_3} & -\frac{(s+k_2)k_1}{k_3} \end{bmatrix} \end{aligned} \tag{A36}$$

As we see, this transfer function is identical to the one found from the state space method (Eq. A28). However, there is no need to find this transfer function since the absolute concentration control matrix $\mathbf{C_{s_i}}(s)$ is found directly as shown in Eq. A6. On the other hand, if a transfer function as Eq. A36 is found from a system identification method, it is not possible to identify the absolute concentration control matrix $\mathbf{C_{s_i}}(s)$ since $\frac{\partial \mathbf{v}}{\partial \mathbf{p}}$ is not invertible.

In order to find the frequency dependent relative concentration control coefficient matrix $\tilde{\mathbf{C}}_{\mathbf{s_i}}(s)$ we use

$$D^{s_i} = \begin{bmatrix} \frac{k_{-2}k_1 + k_1 k_3}{k_3 k_2} & 0 \\ 0 & \frac{k_1}{k_3} \end{bmatrix}, \qquad D^v = \begin{bmatrix} k_1 & 0 & 0 \\ 0 & k_1 & 0 \\ 0 & 0 & k_1 \end{bmatrix}$$

to get

$$\begin{aligned} \tilde{\mathbf{C}}_{\mathbf{s_i}}(s) = & (D^{s_i})^{-1} \cdot \mathbf{C_{s_i}}(s) \cdot D^v \\ = & \frac{1}{s^2 + s(k_2 + k_3 + k_{-2}) + k_3 k_2} \cdot \\ & \begin{bmatrix} \frac{k_2 k_3 (s+k_{-2}+k_3)}{k_{-2}+k_3} & -\frac{k_2 k_3 (s+k_3)}{k_{-2}+k_3} & -\frac{k_2 k_{-2} k_3}{k_{-2}+k_3} \\ k_2 k_3 & k_3 s & -k_3(s + k_2) \end{bmatrix} \end{aligned} \tag{A37}$$

which exhibits robust perfect adaptation from reaction rate v_2 to component I_2. The steady state relative concentration control coefficient matrix becomes:

$$\tilde{\mathbf{C}}_{\mathbf{s_i}} = \begin{bmatrix} 1 & -\frac{k_3}{k_{-2}+k_3} & -\frac{k_{-2}}{k_{-2}+k_3} \\ 1 & 0^{\mathbf{3}} & -1 \end{bmatrix} \tag{A38}$$

Although the dimension of the matrix $\tilde{\mathbf{C}}_{\mathbf{s_i}}$ in Eq. A33 is different from the dimension of $\mathbf{C}^{\mathbf{y}}_{\mathbf{u}}$ in Eq. A38, we note that the sum of the two middle columns in Eq. A33 results in the middle column of Eq. A38.

Fluxes as model output

State space model approach

When the model output is given by the fluxes of the system, the output vector is changed to $\mathbf{y}(t) = [k_1(t),\ k_2(t)x_1(t),\ k_{-2}(t)x_2(t),\ k_3(t)x_2(t)]^T$, giving new C and D matrices for the linearized state space model as

$$C = \begin{bmatrix} 0 & 0 \\ k_2 & 0 \\ 0 & k_{-2} \\ 0 & k_3 \end{bmatrix} \quad D = \begin{bmatrix} 1 & 0 & 0 & 0 \\ 0 & x_1 & 0 & 0 \\ 0 & 0 & x_2 & 0 \\ 0 & 0 & 0 & x_2 \end{bmatrix}$$

Using the steady state expressions given in Eq. A27 together with the steady state expressions for the outputs, i.e. $\mathbf{y_{ss}} = [k_1,\ k_2x_1,\ k_{-2}x_2,\ k_3x_2]^T$, we get the following transfer function matrix $\mathbf{H}(s)$

$$\mathbf{H}(s) = \frac{1}{s^2 + s(k_2 + k_3 + k_{-2}) + k_3k_2} \cdot \begin{bmatrix} 1 & 0 & 0 & 0 \\ k_2(s + k_3 + k_{-2}) & \frac{k_1(k_{-2}+k_3)(s+k_3+k_{-2})s}{k_2k_3} & \frac{k_2k_1(s+k_3)}{k_3} & -\frac{k_2k_{-2}k_1}{k_3} \\ k_2k_{-2} & \frac{k_{-2}k_1(k_{-2}+k_3)}{k_2k_3}s & \frac{k_1(s^2+s(k_2+k_3)+k_2k_3)}{k_3} & -\frac{k_{-2}k_1(s+k_2)}{k_3} \\ k_2k_3, & \frac{k_1(k_{-2}+k_3)}{k_2}s & -k_1s & \frac{sk_1(s+k_{-2}+k_2)}{k_3} \end{bmatrix} \tag{A39}$$

where the frequency dependent relative sensitivity coefficient matrix $\mathbf{C}^{\mathbf{y}}_{\mathbf{u}}(s)$ becomes

$$\mathbf{C}^{\mathbf{y}}_{\mathbf{u}}(s) = \frac{1}{s^2 + s(k_2 + k_3 + k_{-2}) + k_3k_2} \cdot \begin{bmatrix} 1 & 0 & 0 & 0 \\ \frac{(s+k_3+k_{-2})k_2k_3}{k_3+k_{-2}} & s(s + k_3 + k_{-2}) & \frac{(s+k_3)k_{-2}k_2}{k_3+k_{-2}} & \frac{-k_{-2}k_2k_3}{k_3+k_{-2}} \\ k_2k_3 & (k_3 + k_{-2})s & s^2 + s(k_3 + k_2) + k_3k_2 & -(s + k_2)k_3 \\ k_2k_3 & (k_3 + k_{-2})s & -k_{-2}s & s(s + k_{-2} + k_2) \end{bmatrix} \tag{A40}$$

By inspecting the numerator polynomials $n_{u_n}^{y_p}(s)$ of Eq. A40 we find 3 robustly disconnected elements and 5 robust perfectly adapted elements, as indicated in Eq. A41. The only element which is nonzero and frequency independent is the element (1,1), since the output is exactly the same as the input. The $\mathbf{C}_{\mathbf{u}}^{\mathbf{y}}(s)$ matrix in Eq. A40 is presented in terms of Bode plots in Fig. S3 showing a wide range of filtering characteristics, e.g. low-pass in element (2,1), high-pass in element (4,4), band-pass in element (4,2) and all-pass in element (3,3).

A time domain based visualization of the results in element (4,4) is presented in Fig. S4, where both a step and different sinusoidal perturbations in $u_4(t) = k_3(t)$ are plotted together with the output $y_4(t) = J_3(t)$. The high-pass filter characteristics observed as the frequency of sinusoidal perturbation of $k_3(t)$ increases, is due to the fact that the level of the component $x_2(t)$ becomes less and less affected (see element (2,4) in Fig. S2) and therefore exhibit almost steady state behavior at high frequencies. This again implies that the flux $J_3(t)$ which is calculated as $J_3(t) = k_3(t) \cdot x_2(t)$ would follow the sinusoidal behavior of $k_3(t)$ (shown in plot (2,2) of Fig. S4).

The opposite behavior is found when the sinusoidal frequency of $k_3(t)$ approaches zero. Then the level of $x_2(t)$ is highly affected by the variation in $k_3(t)$ (the low frequency amplification of element (2,4) in Fig. S2 is 0 dB, i.e. 1). Simultaneously, the low frequency amplification of element (4,4) in Fig. S3 is $-\infty$dB, i.e. 0, which means that the flux $J_3(t)$ is unaffected by low frequency changes in $k_3(t)$ (shown in plot (1,1) of Fig. S4 using a step).

The steady state relative sensitivity coefficient matrix becomes

$$\mathbf{C}_{\mathbf{u}}^{\mathbf{y}} = \begin{bmatrix} 1 & 0^{\mathbf{1}} & 0^{\mathbf{1}} & 0^{\mathbf{1}} \\ 1 & 0^{\mathbf{3}} & \frac{k_{-2}}{k_3+k_{-2}} & -\frac{k_{-2}}{k_3+k_{-2}} \\ 1 & 0^{\mathbf{3}} & 1 & -1 \\ 1 & 0^{\mathbf{3}} & 0^{\mathbf{3}} & 0^{\mathbf{3}} \end{bmatrix} \tag{A41}$$

where both matrices in Eqs. A40 and A41 satisfies the summation theorem for fluxes.

Stoichiometric network model approach

Using the matrices in Eq. A35, the transfer function $\mathbf{H_v}(s)$ becomes

$$\begin{aligned}\mathbf{H_v}(s) =& \frac{1}{s^2 + s(k_2 + k_3 + k_{-2}) + k_3 k_2} \cdot \\ & \begin{bmatrix} 1 & 0 & 0 & 0 \\ k_2(s + k_3) & \frac{(s+k_3)k_1(k_{-2}+k_3)}{k_2 k_3} s & -\frac{k_1(s+k_3)}{k_3} s & -\frac{k_{-2}k_1}{k_3} s \\ k_2 k_3 & \frac{k_1(k_{-2}+k_3)}{k_2} s & -k_1 s & \frac{k_1(s+k_2+k_{-2})}{k_3} s \end{bmatrix}\end{aligned} \tag{A42}$$

and as we see, this transfer function is *not* identical to one found from the state space approach (Eq. A39). This is due to the lumping of reactions, and thereby different matrix size. In order to find the frequency dependent relative flux control coefficient matrix $\tilde{\mathbf{C}}_\mathbf{v}(s)$ we use

$$D^v = \begin{bmatrix} k_1 & 0 & 0 \\ 0 & k_1 & 0 \\ 0 & 0 & k_1 \end{bmatrix}$$

to get

$$\begin{aligned}\tilde{\mathbf{C}}_\mathbf{v}(s) =& (D^v)^{-1} \cdot \mathbf{C_v}(s) \cdot D^v \\ =& \frac{1}{s^2 + s(k_2 + k_3 + k_{-2}) + k_3 k_2} \cdot \\ & \begin{bmatrix} 1 & 0 & 0 \\ k_2(s + k_3) & (s + k_3)s & k_{-2}s \\ k_2 k_3 & k_3 s & s^2 + (k_2 + k_{-2})s \end{bmatrix}\end{aligned} \tag{A43}$$

From this matrix we identify 2 robustly disconnected elements and 4 robust perfectly adapted elements. The steady state version becomes

$$\tilde{\mathbf{C}}_\mathbf{v} = \begin{bmatrix} 1 & 0^\mathbf{1} & 0^\mathbf{1} \\ 1 & 0^\mathbf{3} & 0^\mathbf{3} \\ 1 & 0^\mathbf{3} & 0^\mathbf{3} \end{bmatrix} \tag{A44}$$

which is, as expected, different from the state space approach results in Eq. A41. It is interesting to note the elements representing the relative flux control coefficient from k_3 to the fluxes J_2 and J_{-2} in Eq. A41, i.e. elements (2,4) and (3,4), do not subtract up to a non-robust perfectly adapted 0 as in Eq. A44, i.e. element (2,3).

In order to obtain the same result as in Eq. A41 by the stoichiometric network approach, the flux v_2 in M2 must be divided into two separate fluxes where the stoichiometric matrix N becomes

$$N = \begin{bmatrix} 1 & -1 & 1 & 0 \\ 0 & 1 & -1 & -1 \end{bmatrix}$$

Motif M3

To show a relative sensitivity coefficient matrix including non-robust perfect adaption sites, we consider the following network,

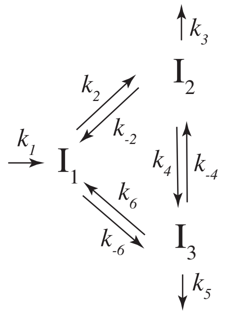

(M3)

studying the cases where either concentrations or fluxes are model outputs.

Concentrations as model output

The input include all the rate constants $\mathbf{u}(t) = [k_1(t), \ldots, k_6(t),\ k_{-2}(t)\ k_{-4}(t),\ k_{-6}(t)]^T$ and the output consists of the concentrations $\mathbf{y}(t) = [x_1(t),\ x_2(t),\ x_3(t)]^T$. In [4] it was found that this network has no zero element in the steady state relative sensitivity matrix $\mathbf{C}_\mathbf{u}^\mathbf{y}$, and hence no robustly disconnected or robust perfectly adapted sites. Furthermore it was found that the network exhibit non-robust perfect adaption from k_4 to the concentration of component I_1 if the following condition $-k_5k_{-2} + k_6k_3 = 0$ is fulfilled.

Inspecting the numerator polynomials of $\mathbf{C}_\mathbf{u}^\mathbf{y}(s)$, two non-robustly perfect adapted sites can be identified, i.e. both from k_4 and k_{-4} to the concentration of component I_1. The numerator polynomial $n_{u_4}^{y_1}(s)$ for element (1,4) of $\mathbf{C}_\mathbf{u}^\mathbf{y}(s)$ is given as

$$n_{u_4}^{y_1}(s) = k_4\bigl(k_2k_{-4} + k_2k_5 + k_2k_6 + k_{-4}k_{-6}\bigr)\bigl((k_6 - k_{-2})s + (k_6k_3 - k_5k_{-2})\bigr) \quad \text{(A45)}$$

where the functions $q(\mathbf{u_{ss}}, \boldsymbol{\alpha})$, $h_1(\mathbf{u_{ss}}, \boldsymbol{\alpha})$ and $h_0(\mathbf{u_{ss}}, \boldsymbol{\alpha})$ from Eq. 16 in main paper are readily identified. From Eq. A45 we see that condition 3a) is already fulfilled, whereas condition 3b) is fulfilled if $q(\mathbf{u_{ss}}, \boldsymbol{\alpha}) \cdot h_1(\mathbf{u_{ss}}, \boldsymbol{\alpha}) \neq 0$, leading to

$$k_4\big(k_2k_{-4} + k_2k_5 + k_2k_6 + k_{-4}k_{-6}\big) \neq 0 \tag{A46}$$

$$k_{-2} \neq k_6 \tag{A47}$$

Condition 3c) *cannot* be fulfilled, but condition 4c) is fulfilled since there exists a solution to $h_0(\mathbf{u_{ss}}, \boldsymbol{\alpha}) = 0$ which is:

$$k_5k_{-2} = k_6k_3 \tag{A48}$$

Hence, scenario 4 of non-robust perfect adaptation can be observed. The steady state relative sensitivity coefficient matrix $\mathbf{C_u^y}$ for an arbitrary set of chosen rate constants which fulfills only condition 3b), e.g. $\mathbf{u}_{ss} = [1, 2, 3, 4, 5, 6, 7, 8, 9]$ (the parameter vector $\boldsymbol{\alpha}$ is empty), becomes:

$$\mathbf{C_u^y} = \begin{bmatrix} 1 & -0.15 & -0.22 & -0.03^{\mathbf{4}} & -0.40 & 0.32 & 0.25 & 0.08^{\mathbf{4}} & -0.84 \\ 1 & 0.19 & -0.46 & -0.22 & -0.61 & 0.07 & -0.31 & 0.53 & -0.19 \\ 1 & -0.09 & -0.26 & 0.11 & -0.70 & -0.03 & 0.15 & -0.26 & 0.09 \end{bmatrix}$$

satisfying the summation theorem for fluxes.

If we model the same system as a stoichiometric network where the reversible reactions are lumped together to v_2, v_4 and v_6, the numerator $n_{u_4}^{y_1}(s)$ of element (1,4) of the relative/scaled frequency dependent concentration control coefficient matrix $\tilde{\mathbf{C}}_{\mathbf{s_i}}(s)$ becomes

$$n_{u_4}^{y_1}(s) = \big(k_2k_4(k_5 + k_6) - k_{-4}k_{-6}(k_{-2} + k_3)\big)\big((k_6 - k_{-2})s + (k_6k_3 - k_5k_{-2})\big) \tag{A49}$$

where condition 2b) is fulfilled since there exists a solution to $q(\mathbf{u_{ss}}, \boldsymbol{\alpha}) = 0$ which is:

$$k_2k_4(k_5 + k_6) = k_{-4}k_{-6}(k_{-2} + k_3) \tag{A50}$$

Hence, the concentration of component I_1 is non-robustly disconnected to changes in v_4 (i.e. both k_4 and k_{-4} changes simultaneously). The function $q(\mathbf{u_{ss}}, \boldsymbol{\alpha})$ from Eq. A49 also appears in the elements (2,4) and (3,4) of $\tilde{\mathbf{C}}_{\mathbf{s_i}}(s)$.

By choosing $\mathbf{u}_{ss} = [1, 2, 3, 4, 5, 5, 7, 8, 1]$ the conditions 2b) and 2c) are fulfilled, whereas the condition 4c) (Eq. A48) is not. Hence, from the state space approach, the relative sensitivity coefficient matrix $\mathbf{C_u^y}(s)$ indicates that these parameter values do not lead to any kind of perfect adaptation

$$\mathbf{C}_{\mathbf{u}}^{\mathbf{y}} = \begin{bmatrix} 1 & -0.61 & -0.36 & -0.06^{\mathbf{4}} & -0.26 & 0.19 & 0.43 & 0.06^{\mathbf{4}} & -0.38 \\ 1 & 0.21 & -0.61 & -0.25 & -0.35 & 0.10 & -0.14 & 0.25 & -0.21 \\ 1 & -0.25 & -0.47 & 0.30 & -0.58 & -0.12 & 0.17 & -0.30 & 0.25 \end{bmatrix} \tag{A51}$$

whereas the steady state relative concentration coefficient matrix $\tilde{\mathbf{C}}_{\mathbf{s_i}}(s)$ indicates that all three concentrations are non-robustly disconnected to the input v_4

$$\tilde{\mathbf{C}}_{\mathbf{s_i}} = \begin{bmatrix} 1 & -0.18 & -0.36 & 0^{\mathbf{2}} & -0.26 & -0.19 \\ 1 & 0.06 & -0.61 & 0^{\mathbf{2}} & -0.35 & -0.10 \\ 1 & -0.07 & -0.47 & 0^{\mathbf{2}} & -0.58 & 0.12 \end{bmatrix} \tag{A52}$$

We see that the sum of column 4 and 8 in Eq. A51 is $[0,0,0]^T$, and hence, explains the non-robust disconnection from v_4 to the concentrations in Eq. A52.

Fluxes as model output

Now, using the fluxes as model output and the same values for $\mathbf{u_{ss}}$ as in the previous example, i.e. $\mathbf{u}_{ss} = [1,2,3,4,5,5,7,8,1]$, some of the elements of the relative flux control coefficient matrix $\tilde{\mathbf{C}}_{\mathbf{v}}$ actually contains the function $q(\mathbf{u_{ss}}, \boldsymbol{\alpha})$ from Eq. A49 in the *denominator*, producing the following result

$$\tilde{\mathbf{C}}_{\mathbf{v}} = \begin{bmatrix} 1 & 0^{\mathbf{1}} & 0^{\mathbf{1}} & 0^{\mathbf{1}} & 0^{\mathbf{1}} & 0^{\mathbf{1}} \\ 1 & 0.24 & 0.21 & 0^{\mathbf{2}} & -0.05 & -0.41 \\ 1 & 0.06 & 0.39 & 0^{\mathbf{2}} & -0.35 & -0.10 \\ 1 & \infty & \infty & 0.45 & \infty & \infty \\ 1 & -0.07 & -0.47 & 0^{\mathbf{2}} & 0.42 & 0.12 \\ 1 & -0.29 & -0.25 & 0^{\mathbf{2}} & 0.06 & 0.49 \end{bmatrix} \tag{A53}$$

where some elements actually becomes infinity. The corresponding relative sensitivity coefficient matrix $\mathbf{C}_{\mathbf{u}}^{\mathbf{y}}(s)$ from the state space approach is

$$\mathbf{C}_{\mathbf{u}}^{\mathbf{y}} = \begin{bmatrix} 1 & 0^{\mathbf{1}} & 0^{\mathbf{1}} & 0^{\mathbf{1}} & 0^{\mathbf{1}} & 0^{\mathbf{1}} & 0^{\mathbf{1}} & 0^{\mathbf{1}} & 0^{\mathbf{1}} \\ 1 & 0.39 & -0.36 & -0.07 & -0.26 & 0.19 & 0.43 & 0.07 & -0.39 \\ 1 & 0.21 & 0.39 & -0.25 & -0.35 & 0.10 & -0.14 & 0.25 & -0.21 \\ 1 & 0.21 & -0.61 & 0.75 & -0.35 & 0.10 & -0.14 & 0.25 & -0.21 \\ 1 & -0.25 & -0.47 & 0.30 & 0.42 & -0.12 & 0.17 & -0.30 & 0.25 \\ 1 & -0.25 & -0.47 & 0.30 & -0.58 & 0.88 & 0.17 & -0.30 & 0.25 \\ 1 & 0.21 & -0.61 & -0.25 & -0.35 & 0.10 & 0.86 & 0.25 & -0.21 \\ 1 & -0.25 & -0.47 & 0.30 & -0.58 & -0.12 & 0.17 & 0.70 & 0.25 \\ 1 & -0.61 & -0.36 & -0.07 & -0.26 & 0.19 & 0.43 & 0.07 & 0.61 \end{bmatrix}$$

where such infinity elements are avoided. Hence, we argue that the modeling in general should not include lumping of reactions when relative sensitivity coefficients are to be found. This argument is supported by the fact that a step can in fact be applied to only one of the reactions in an reversible reaction (as shown in [4]), and there is a need to separate the reactions.

References

[1] Ingalls, B. P. *J. Phys. Chem. B* **2004**, *108*, 1143–1152.

[2] Reder, C. *J Theor Biol* **1988**, *135*, 175–210.

[3] Hofmeyr, J. H. S. In Yi, T. M., Hucka, M., Morohashi, M., Kitano, H., Eds., *Proceedings of the 2nd International Conference on Systems Biology*, pages 291–300. Omnipress, 2001.

[4] Drengstig, T.; Ueda, H. R.; Ruoff, P. *J Phys Chem B* **2008**, *112*, 16752–16758.

Figure Legends

Figure S1.

Response in the fluxes of motif M1 for a step-wise increase in temperature from 308K to 318K at time $t = 1$. The parameters values are $\boldsymbol{\alpha} = [A_1, \ldots, A_6, E_1, \ldots, E_6, R]$ where the vector of activation constants are $[A_1, \ldots, A_6] = [1.0274,\ 2.0276,\ 3.1488,\ 4.0356,\ 5.2017,\ 6.0291]$, activation energies $[E_1, \ldots, E_6] = [67, 34, 120, 22, 98, 12]$ and $R = 8.314$. Figure element (2,3) is the same as in Fig. 1 in main paper.

Figure S2.

Bode-plot (magnitude only) of the frequency dependent relative sensitivity coefficient matrix $\mathbf{C}_{\mathbf{u}}^{\mathbf{y}}(s)$ of motif M2 when the output is concentration, using $k_1 = 1.1$, $k_2 = 1.2$, $k_{-2} = 1.3$ and $k_3 = 1.4$.

Figure S3.

Bode-plot (magnitude only) of the frequency dependent relative sensitivity coefficient matrix $\mathbf{C}_{\mathbf{u}}^{\mathbf{y}}(s)$ of motif M2 when the output is flux, using $k_1 = 1.1$, $k_2 = 1.2$, $k_{-2} = 1.3$ and $k_3 = 1.4$.

Figure S4.

Response to a step perturbation (upper left panel) and 3 examples of responses in $y_4(t) = J_3(t)$ to sinusoidal variations in $u_4(t) = k_3(t) = \sin(\omega t)$, i.e. element (4,4) of the frequency dependent relative sensitivity coefficient matrix $\mathbf{C}_{\mathbf{u}}^{\mathbf{y}}(s)$ of motif M2, using $k_1 = 1.1$, $k_2 = 1.2$, $k_{-2} = 1.3$ and $k_3 = 1.4$. Note the different time scales.

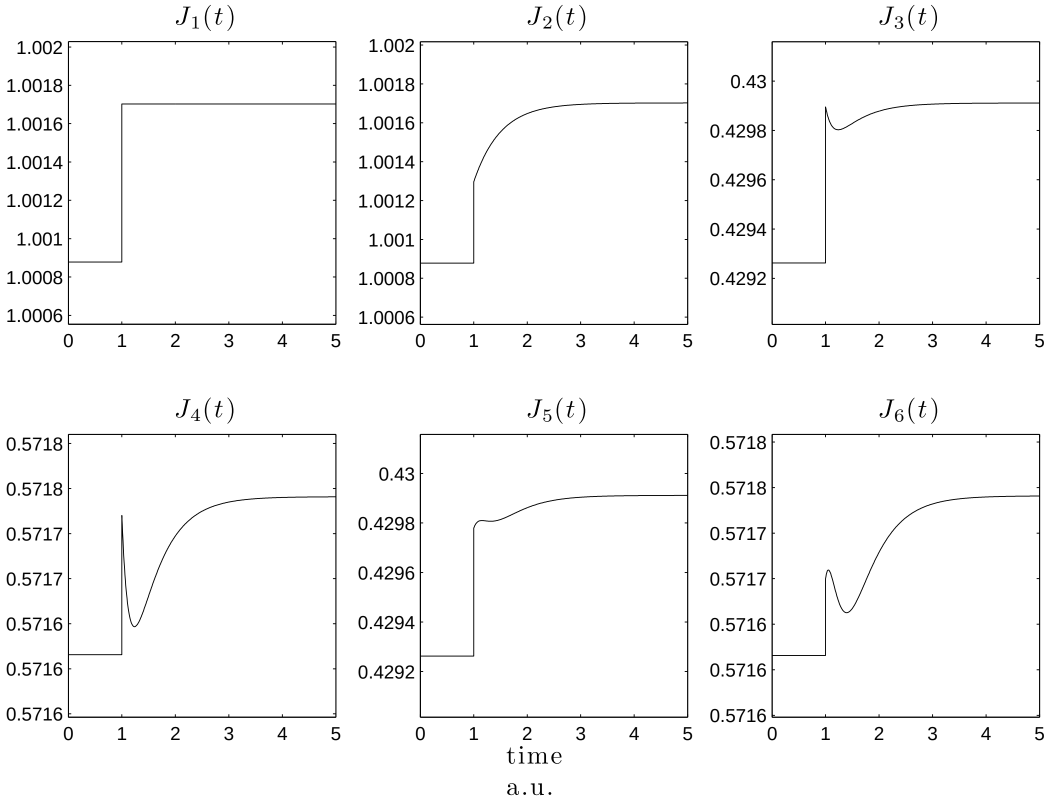
$J_1(t)$
1.002
1.0018
1.0016
1.0014
1.0012
1.001
1.0008
1.0006
0 1 2 3 4 5
$J_2(t)$
1.002
1.0018
1.0016
1.0014
1.0012
1.001
1.0008
1.0006
0 1 2 3 4 5
$J_3(t)$
0.43
0.4298
0.4296
0.4294
0.4292
0 1 2 3 4 5
$J_4(t)$
0.5718
0.5718
0.5717
0.5717
0.5716
0.5716
0.5716
0 1 2 3 4 5
$J_5(t)$
0.43
0.4298
0.4296
0.4294
0.4292
0 1 2 3 4 5
$J_6(t)$
0.5718
0.5718
0.5717
0.5717
0.5716
0.5716
0.5716
0 1 2 3 4 5
time
a.u.

Figure S1:

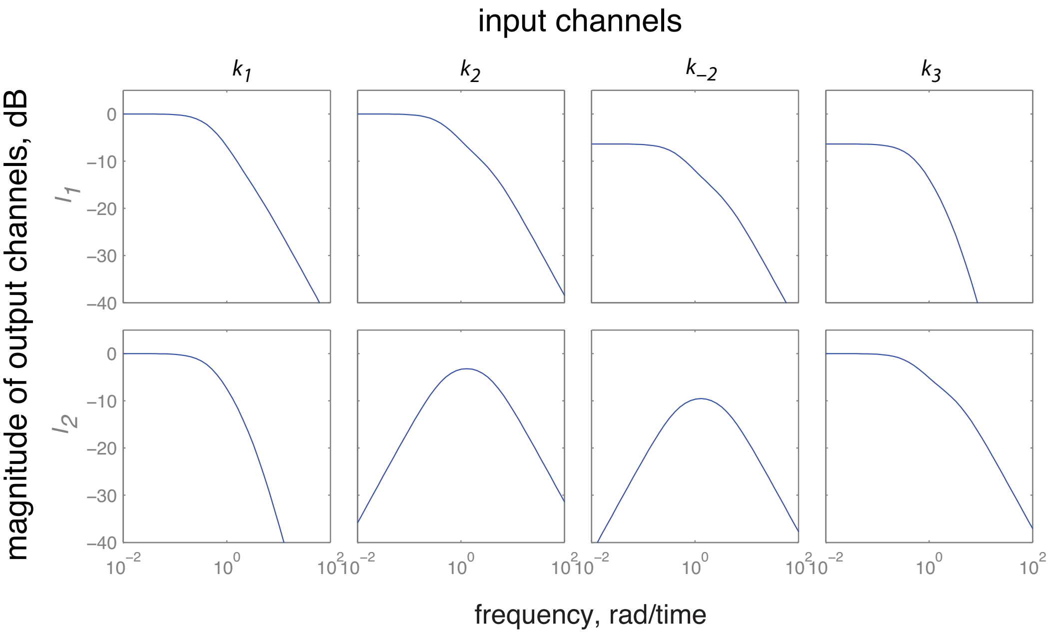
input channels
k1
k2
k−2
k3
magnitude of output channels, dB
l1
l2
0
−10
−20
−30
−40
10^−2
10^0
10^2
frequency, rad/time

Figure S2:

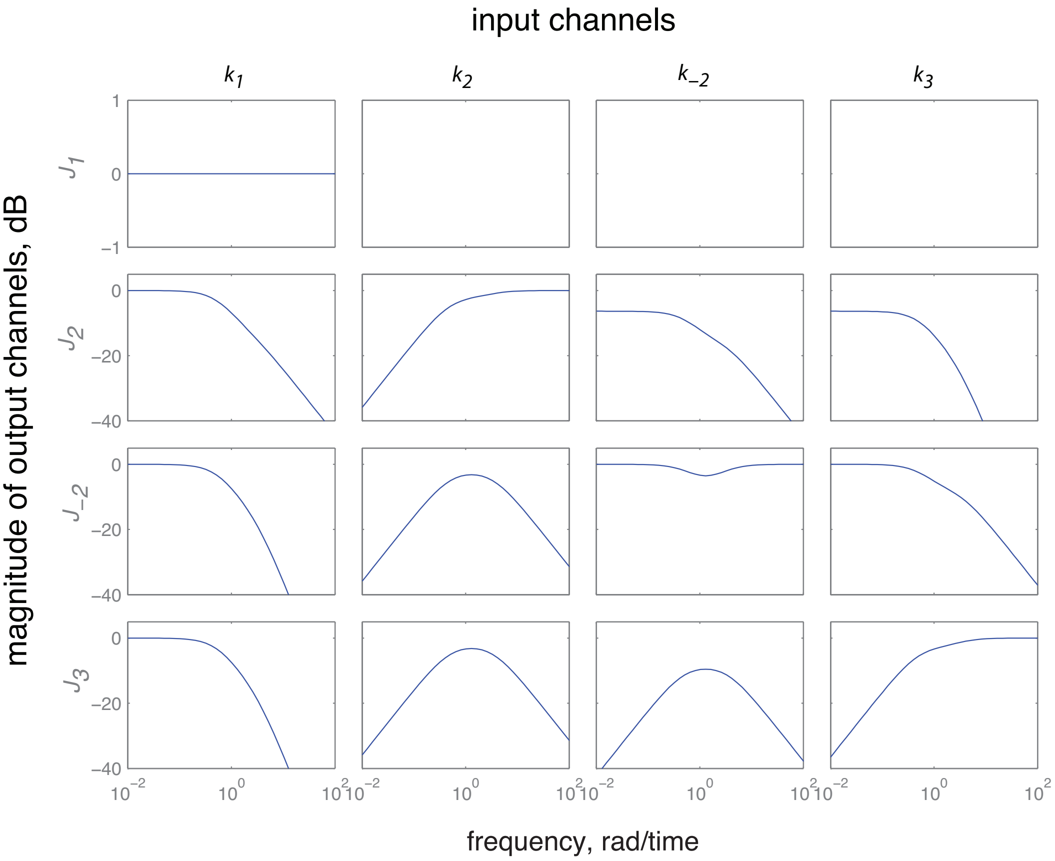
input channels
k_1
k_2
k_{-2}
k_3
magnitude of output channels, dB
J_1
J_2
J_{-2}
J_3
1
0
−1
0
−20
−40
10^{-2}
10^{0}
10^{2}
frequency, rad/time

Figure S3:

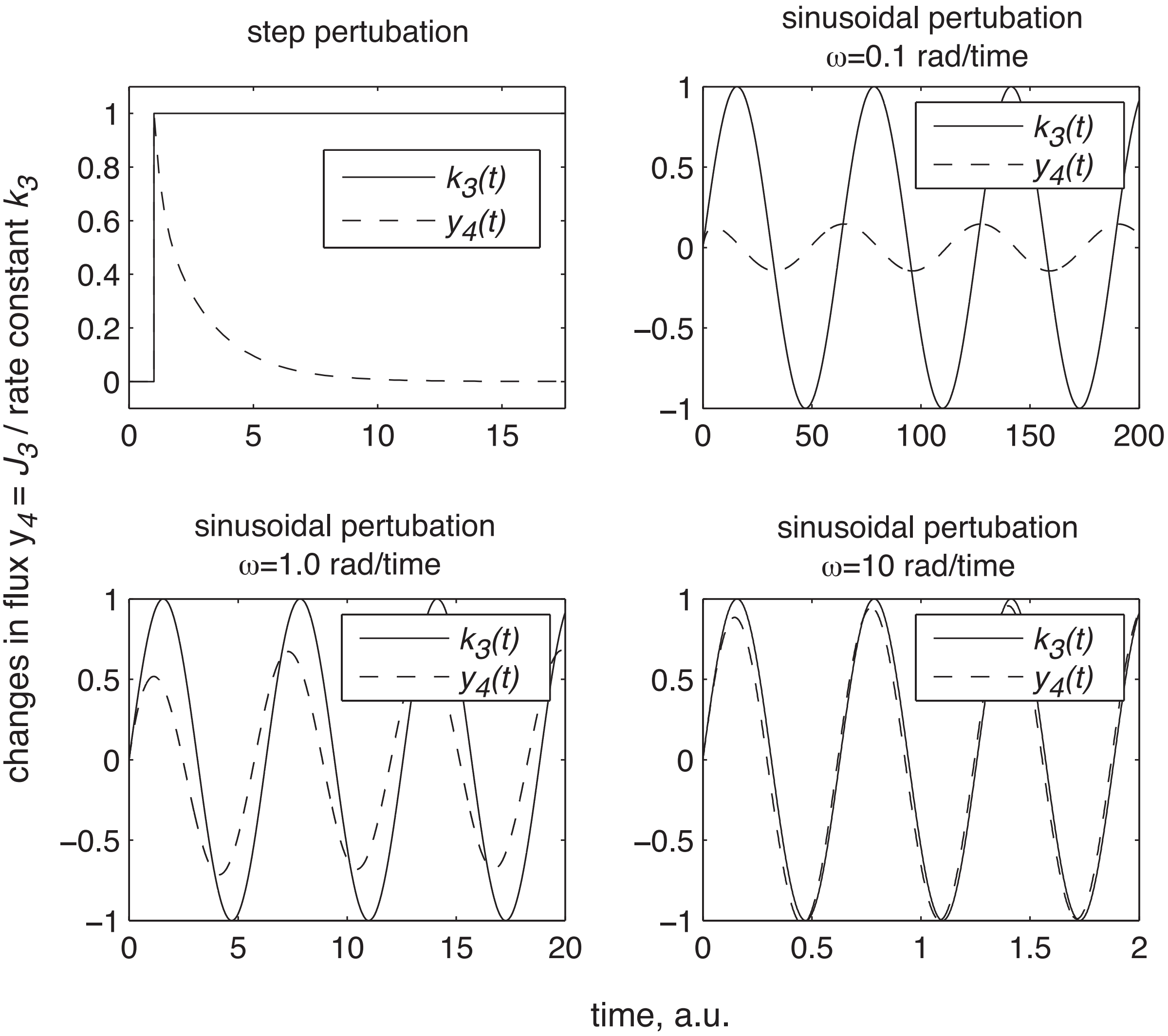
step pertubation
sinusoidal pertubation
ω=0.1 rad/time
sinusoidal pertubation
ω=1.0 rad/time
sinusoidal pertubation
ω=10 rad/time
$k_3(t)$
$y_4(t)$
changes in flux $y_4 = J_3$ / rate constant k_3
time, a.u.
0
0.2
0.4
0.6
0.8
1
5
10
15
20
50
100
150
200
0.5
1.5
2
−0.5
−1

Figure S4: